Available online at www.sciencedirect.com
ScienceDirect
ELSEVIER
Surface Science 601 (2007) 3892–3897
SURFACE SCIENCE
www.elsevier.com/locate/susc

Structural and optical properties of an $In_xGa_{1-x}N/GaN$ nanostructure

Sabit Korçak [a], M. Kemal Öztürk [a], Süleyman Çörekçi [a], Barış Akaoğlu [a], Hongbo Yu [b], Mehmet Çakmak [a], Semran Sağlam [a], Süleyman Özçelik [a,*], Ekmel Özbay [b]

[a] Department of Physics, Gazi University, Teknikokullar, 06500 Ankara, Turkey
[b] Nanotechnology Research Center, Bilkent University, 06800 Ankara, Turkey

Available online 19 April 2007

Abstract

The structural and optical properties of an $In_xGa_{1-x}N/GaN$ multi-quantum well (MQW) were investigated by using X-ray diffraction (XRD), atomic force microscopy (AFM), spectroscopic ellipsometry (SE) and photoluminescence (PL). The MQW structure was grown on *c*-plane (0001)-faced sapphire substrates in a low pressure metalorganic chemical vapor deposition (MOCVD) reactor. The room temperature photoluminescence spectrum exhibited a blue emission at 2.84 eV and a much weaker and broader yellow emission band with a maximum at about 2.30 eV. In addition, the optical gaps and the In concentration of the structure were estimated by direct interpretation of the pseudo-dielectric function spectrum. It was found that the crystal quality of the InGaN epilayer is strongly related with the Si doped GaN layer grown at a high temperature of 1090 °C. The experimental results show that the growth MQW on the high-temperature (HT) GaN buffer layer on the GaN nucleation layer (NL) can be designated as a method that provides a high performance InGaN blue light-emitting diode (LED) structure.
© 2007 Elsevier B.V. All rights reserved.

Keywords: Metalorganic chemical vapor deposition; $In_xGa_{1-x}N/GaN$; X-ray reflectivity; Photoluminescence; Atomic force microscopy; Ellipsometry

1. Introduction

Current intensive research on III nitrides has led to rapid progress in optoelectronic devices such as blue/green light-emitting diodes (LEDs), laser diodes (LDs) and high power electronic devices [1,2]. The performance of the devices primarily depend on the magnitude of lattice mismatch at heterojunctions, dislocation density, interface roughness (sharpness) and in turn, localized states in the InGaN quantum wells which critically affect optical and especially, electronic properties of the devices. In order to investigate the material quality in terms of structural and optical properties under several growth procedures of the III-nitrides compounds, characterization techniques such as X-ray reflectivity (XRR), high-resolution X-ray diffractions (HXRD), atomic force microscopy (AFM), photoluminescence (PL) and spectroscopic ellipsometry (SE) are widely used [3–8]. To improve the performance of nitride-based optoelectronic and microelectronic devices, various growth procedures have been employed which indicates that a better knowledge of their growth kinetics, surface dynamics and lattice structures is necessary. Among the various efforts for this purpose, the growth of the layers on the buffer and the quantum well (QW) at particular temperatures is quite critical for device characteristics due to modification of lattice structure and band gap. Several groups have studied the effects of such layers on the optical and structural properties of $In_xGa_{1-x}N/GaN$ MQWs [9–16].

In this study, we demonstrate that a high quality $In_xGa_{1-x}N/GaN$ heterostructure can be grown by introducing a high-temperature (HT) Si doped GaN thick layer and a HT-GaN buffer layer between MQW structure and low-temperature (LT) nucleation layer (NL). The results are interpreted in terms of interface and crystalline qualities of the MQW. The structural properties were studied by

* Corresponding author. Tel.: +90 312 2021242; fax: +90 312 2122279.
E-mail address: sozcelik@gazi.edu.tr (S. Özçelik).

0039-6028/$ - see front matter © 2007 Elsevier B.V. All rights reserved.
doi:10.1016/j.susc.2007.04.088

HXRD and AFM technique and the optical properties have been investigated by PL and SE. In addition, the surface and interface roughness were investigated by XRR technique.

2. Experimental procedure

The $In_xGa_{1-x}N$ MQW was grown by MOCVD on a *c*-plane (0001)-faced sapphire substrate with a 100 nm-thick LT-GaN nucleation layer. During the growth, the reactor pressure was maintained at 200 mbar. Prior to the growth of MQW, a HT-GaN buffer layer with a thickness of 700 nm was deposited at 1050 °C and then a n-type GaN:Si layer of thickness 250 nm was grown at 1090 °C. The sample contains five periods of 4-nm $In_xGa_{1-x}N$ active layer that is grown on a thin 16-nm GaN grown at 710 °C. The cap layer was capped with a 200-nm-thick p-type GaN:Mg grown at 1030 °C. Fig. 1a shows the schematically drawing of the above mentioned structure and the target values of the thickness are presented in the brackets.

The XRD and reciprocal space mapping (RSM) measurement were performed using a D8/Bruker diffractometer, equipped on the primary side with a Ge(022) monochromator. Surface morphology was observed by AFM using an Omicron VT (variable temperature) STM/AFM instrument at room temperature and atmosphere pressure. SE measurements were performed by an UVISEL variable angle spectroscopic phase modulated ellipsometer (Jobin Yvon-Horiba) with a spectral range 0.59–4.7 eV. The orientations of the analyzer and modulator were set to 45° and 0°, respectively. In this configuration, the system measures $I_s = \sin(2\psi)\sin(\Delta)$ and $I_c = \sin(2\psi)\cos(\Delta)$ where ψ and Δ are conventional ellipsometric angles [17]. 55 mW He–Cd laser (325 nm) is used as a light source in room temperature PL measurements.

3. Results and discussion

The MQW structure is presented with the measured structural properties by HXRD in Fig. 1a. When a GaN epilayer is desired to be grown on sapphire substrates, it is necessary to grow a thin GaN NL at low temperature of about 500 °C due to a large lattice-mismatch up to 13.6% between GaN and sapphire. Then, the growth temperature is subsequently raised to more than about 1050 °C to grow a thick GaN buffer layer prior to the growth of any device structure. During the subsequent high-temperature (HT) growth, the HT islands are initially expected to be formed, and then laterally coalescence occurs which finally leads to an atomically flat surface [18].

X-ray reflectivity scan for the azimuth orientation of the sample was performed using Cu (1.54 Å) radiation as shown in Fig. 1b. In principle, the thicknesses of the layers, their chemical composition as well as the root mean square (rms) roughness of the interfaces can be obtained from such measurements. As shown in the Fig. 1b, the plateau region in the about 0–0.7° interval is strongly smooth which suggests that the sample surface is uniform. The measured reflection curve exhibits an exponential behavior and gives the satellite peaks up to SL + 5th order. In the reflectivity curve, no clear satellite (SL) peaks were observed because the height of the satellite is strongly influenced by the interface roughness, and by the thickness of the individual layers building up the multilayer period. There is a strong contribution of a background that also depends on the sample orientation. After subtracting a diffuse background, the period D of the stack is determined to be $D = d_{\text{well}} + d_{\text{barrier}} = (17.9 \pm 0.5)$ nm with $\sigma = d_{\text{well}} + d_{\text{barrier}} = (1.6 \pm 0.1)$ nm rms roughness. Relatively higher degree of roughness affects the satellite oscillation in the reflectivity curve and particularly, its amplitude decreases.

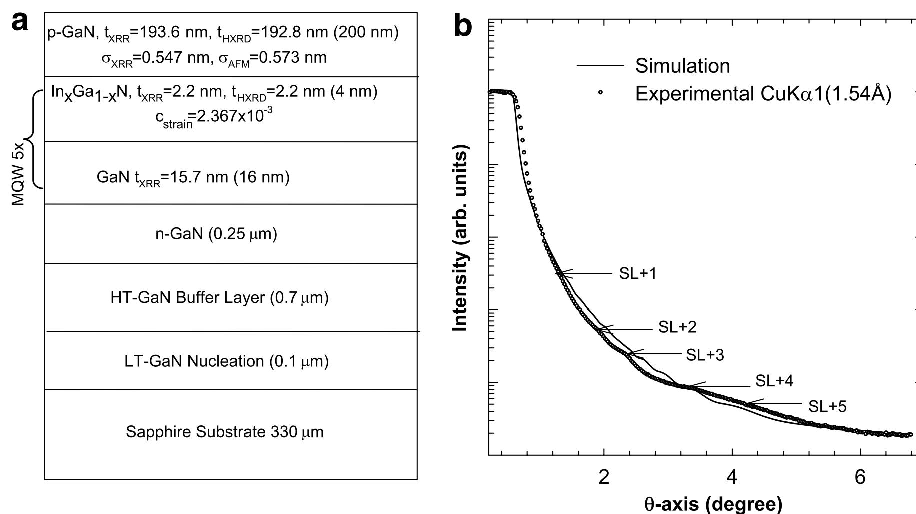

Fig. 1. (a) The schematic representation and structural properties of the MQW structure. Values within the bracket show the nominal values of the layers. (b) The reflectivity of the 5× MQW sample. Arrows point the satellite peaks.

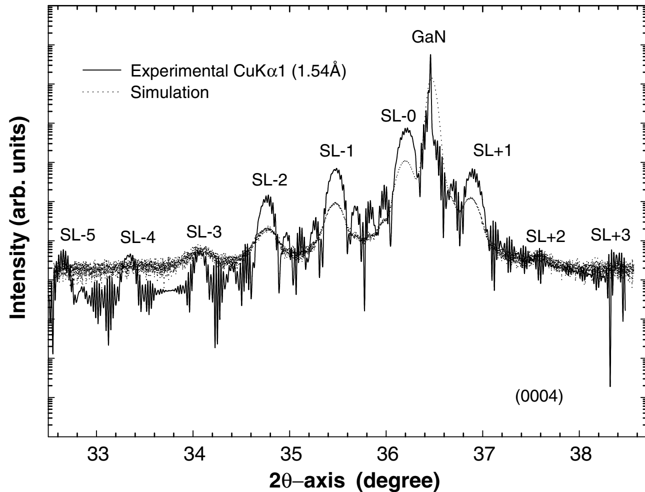

Fig. 2. The 2θ-axis scan for the (004) reflection of the 5× MQW sample.

Reflectivity measurements were simulated by the LEPTOS program [19], which is supported by the simulated annealing method.

In Fig. 2, we present the ω–2θ scan curve for the symmetrical (004) Bragg reflection along the (110) azimuth. In this figure, the simulation of an HXRD scan using the LEPTOS program that is based on the solution of the Takagi–Taupin equations of the dynamical diffraction theory is also shown [20]. High order satellites up to SL + 3th and SL − 5th orders can be clearly distinguished, which indicate very good InGaN/GaN interfaces. The GaN peak localized at an angle of 36.410° is very sharp, whereas all the satellite bands are narrow. Finer structures are seen between the satellite peaks. This indicates quite good crystallinity [16]. However, the fringes between satellites are not clearly resolved. Therefore, no information about the layer roughnesses is obtained. Also normal lattice mismatch ratio perpendicular to the sample surface is found to be 2.367×10^{-3} by using GaN and InN lattice parameters. Using the LEPTOS program, the well width, barrier width and indium composition were estimated to be approximately as 2.2 nm, 15.7 nm and 9.6%, respectively.

Fig. 3a and b shows the typical XRD rocking curves of the GaN buffer in (002) and (102) scan modes. XRD symmetric (002) incorporated with asymmetric (102) scan is a reliable technique to characterize the crystal quality of GaN films [21]. The defects within the structure of the sample cause significant broadening in both the symmetric (002) and asymmetric (102) rocking curves, which have been fitted with widths of 309.6 and 450 arcsec, respectively. It is noteworthy that the measured width of the

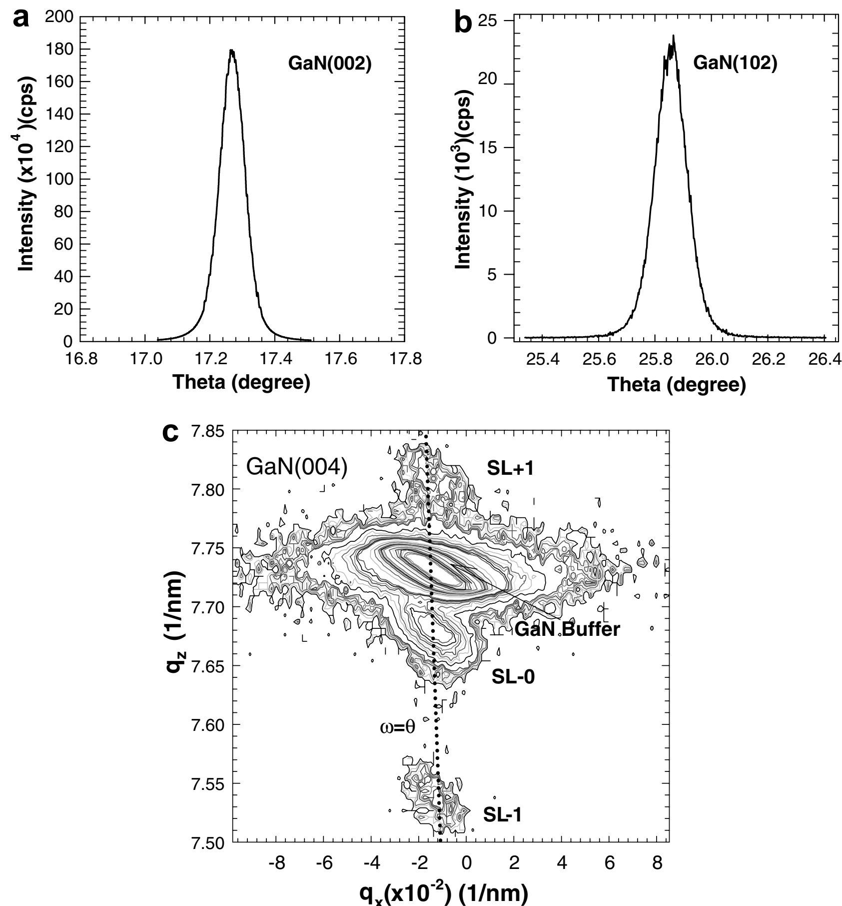

Fig. 3. (a,b) XRD rocking curves of the GaN film used the in (002) and (102) scan modes. (c) Reciprocal space map of the (004) reflection of the 5× MQW sample on GaN/c-sapphire. The $\omega = \theta$ line corresponds to the scan in Fig. 2.

(1 0 2) rocking curve is larger than that of the (0 0 2) rocking curve. The broadening of the asymmetric diffractions compared to the symmetric diffractions is indicative of a defective structure with a large pure edge threading dislocation (TD) content, since the (0 0 2) peak is only broadened by screw or mixed TD while the (1 0 2) peak is broadened by all of the TDs. It is very likely that the high-density edge-type TDs compensate the background of GaN for our sample, leading to the semi-insulating electrical character [22].

The reciprocal map for a (0 0 2) diffraction of the (In, Ga)N quantum well structure is shown in Fig. 3c. The intensity maxima of the GaN buffer layer and the MQW system is set along the line $\omega = \theta$, indicating that the MQW is uniform with respect to the GaN buffer layer. This result is in consistent with the XRR and HXRD results. Along the ω–2θ-direction ($q_\perp$-direction), strain variation and thickness fluctuations of the SL can be seen clearly along the growth direction in the figure. In the ω-direction ($q_\parallel$), it is apparent that the structure peaks exhibit some spreading mosaic pattern with an area of which considerably increases for the higher SL.

AFM images with a $5 \times 5\ \mu m^2$ scan area of the $In_xGa_{1-x}N$-MQW sample are shown in Fig. 4. There are randomly oriented terrace steps, and dark spots on the GaN surface of the sample. However, nano pipes and GaN droplets were not observed. If it is reminded that the atomic step-flow growth mode allows for fast adatom diffusion to the intrinsic steps [23], the parallel and straight terraces, as seen in Fig. 4, suggest a typical step-flow morphology or growth mode. This correlates with the usual growth conditions of the epitaxial GaN [24,25]. In addition, the average step height over the measured region is 0.25 nm, which is close to the height of one monolayer of (0 0 2) GaN. The many terrace steps shown on the GaN surface are pinned, generally appearing as dark spots in the AFM images [26]. The pinned steps should be associated with the screw TDs since a pinned step must be formed when a TD with a screw component intersects a free crystal surface and causes a surface displacement that is normal to the surface. The dislocation density of the GaN cap layer is found to be in the order of $10^8\ cm^{-2}$, by simply counting the dark spots at the edge of steps. This is in agreement with previously reported results [26,27]. The surface roughness was closely related to lateral step size dimension on the surface. The maximum step size on the GaN surface was 400 nm, whereas the average lateral step size on the GaN surface was approximately 250 nm. On the other hand, rms roughness is an important parameter to the definite surface/interface roughness. The GaN surface was found to be flat with a rms roughness of 0.573 nm. The results obtained from both AFM and X-ray measurements are in perfect agreement for the GaN cap surface as seen in Fig. 1a.

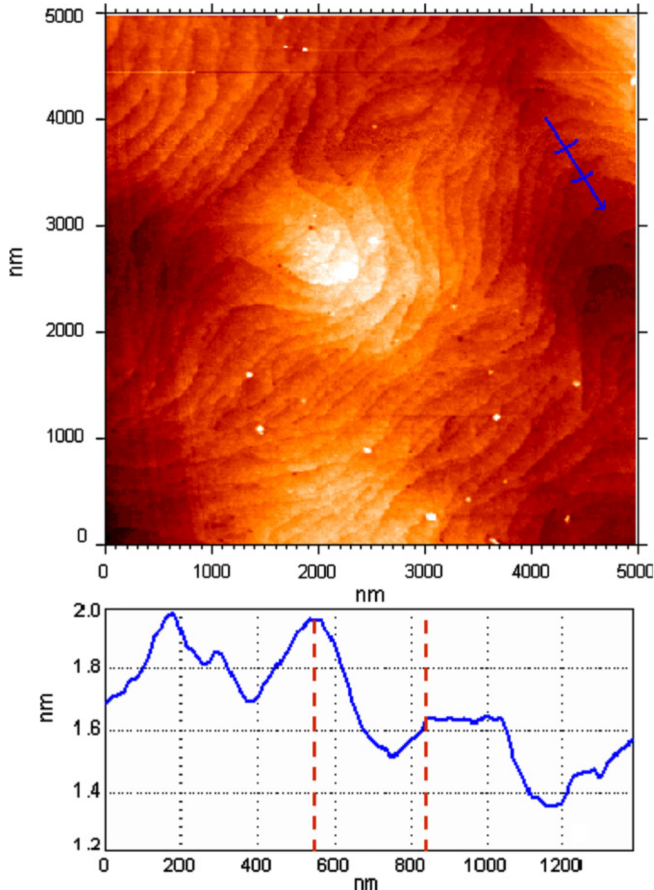

Fig. 4. AFM image of the cap layer (GaN) grown on MWQ.

Pseudo-dielectric function ($\varepsilon = \varepsilon_1 + i\varepsilon_2$) [17] of the MQW structure, obtained from SE measurement, displays the optical gaps (Eg) of the $In_xGa_{1-x}N$ and GaN in Fig. 5a. Due to the multiple transmissions and reflections in the GaN layers, the optical gap of the $In_xGa_{1-x}N$ layer is less apparent; in other words, sharp absorption resonance behavior was destroyed by the Fabry–Perot interference fringes. The modulation of the fringes is due to the uniaxial anisotropic nature of the backside-polished sapphire substrate with a thickness of 330 μm. We determined the optical gap the $In_xGa_{1-x}N$ layers as 2.86 eV within the frame of Kramers–Kronig consistency of optical constants which requires that the energy point at which the ε_1 spectrum exhibits an extremum point corresponds to an extremum point in the ε_2 spectrum, that is, absorption edge. In concentration was estimated as $x = 0.12 \pm 0.02$ using a bowing parameter of 3.8 eV (for $In_xGa_{1-x}N$ with $x = 0.1$) [28]. The x values obtained from both XRD and SE measurements are more or less in agreement within their error limits.

Photoluminescence spectrum of the MQW structure at room temperature is shown in Fig. 5b. A strong blue emission (main peak) at 2.86 eV and a much weaker and broader yellow emission band with a maximum of about 2.3 eV was observed. The shoulder-like behaviour in the main peak is purely an interference effect. The appearance of the yellow band might be due to a number of reasons; a systematic and detailed analysis is necessary, which is out of the scope of this study. However, it was reported that

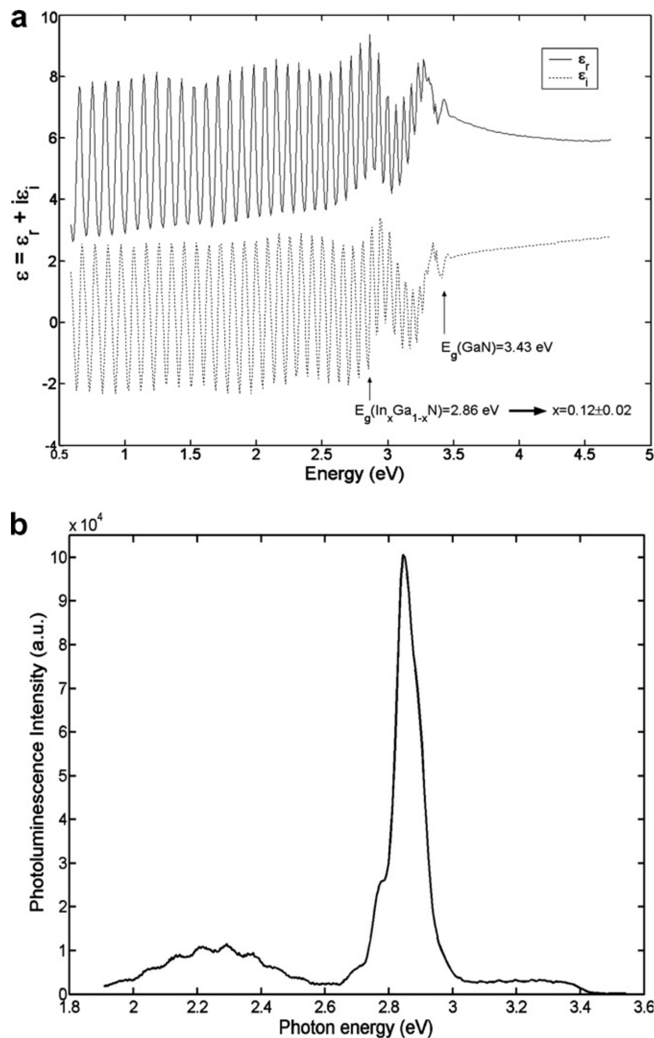

Fig. 5. (a) Real and imaginary parts of pseudo-dielectric function as a function of photon energy obtained from ellipsometry measurements. (b) Photoluminescence spectrum of the MQW structure.

origin of the enhanced yellow emission inside the defects is deep gap states formed by Ga-impurity complex, which are trapped at the side faces [14]. Nevertheless, the fringes appearing in the low energy region exhibit the quality of the grown structure in terms of the homogeneity and regular deposition of the individual layers.

4. Conclusion

The MQW structure grown by MOCVD was investigated by different characterization methods (XRD, PL, SE and AFM) in detail. From the X-ray measurements we obtained the period thicknesses, rms roughness and Indium content of the active layer and all obtained thickness values are in quite agreement with their nominal values. From the HXRD measurements, a weak tetragonally distorted structure was found with a lattice mismatch ratio of 2.367×10^{-3} and an indium concentration of 9.60% in the InGaN/GaN structure. The reciprocal map of the MQW structure indicates that MQW is very uniform which is in agreement with the other results. AFM measurement suggests a step-flow morphology for the GaN surface and the dislocation density is found to be in the order of 10^8 cm^{-2}. In addition, SE and PL measurements do not only give additional information about optical gap and In content of the active layer but also demonstrate the optical and crystalline quality of the grown structure. Consequently, our results show that the growth of MQW on sapphire with HT Si-doped GaN layer on HT buffer layer can be designated as a method that provides a high quality InGaN MQW structure.

Acknowledgements

This work was supported by the Turkish Prime Ministry State Planning Agency under Projects No. 2001K120590, 2003K120470-15 (S.Ö.), and by TUBITAK under Projects No. 104E090, 105E066. One of the authors (E. Ozbay) acknowledges partial support from the Turkish Academy of Sciences.

References

[1] Z. Dridi, B. Bouhafs, P. Ruterana, Semicond. Sci. Technol. 18 (2003) 850.
[2] J.P. Liu, G.D. Shen, J.J. Zhu, S.M. Zhang, D.S. Jiang, H. Yang, J. Crystal Growth 295 (2006) 7.
[3] U. Pietsch, V. Holý, T. Baumbach, High-Resolution X-ray Scattering: From Thin Films to Lateral Nanostructures, Second ed., Springer, 2004.
[4] G. Binnig, C.F. Quate, Ch. Gerber, Phys. Rev. Lett. 56 (1986) 930.
[5] Y. Narukawa, Y. Kawakami, M. Funato, S. Fujita, S. Nakamura, Appl. Phys. Lett. 70 (1997) 981.
[6] N.A. El-Masry, E.L. Piner, S.X. Liu, S.M. Bedair, Appl. Phys. Lett. 72 (1998) 40.
[7] M.H. Lee, K.J. Kim, E. Oh, Solid State Commun. 123 (2002) 395.
[8] J. Wagner, A. Ramakrishnan, D. Behr, M. Maier, N. Herres, M. Kunzer, H. Obloh, K.-H. Bachem, MRS Internet J. Nitride Semicond. Res. 4S1 (1999) G2.8.
[9] X.H. Zheng, H. Chen, Z.B. Yan, H.B. Yu, D.S. Li, Y.J. Han, Q. Huang, J.M. Zhou, J. Crystal Growth 257 (2003) 326.
[10] H. Yu, M.K. Ozturk, S. Ozcelik, E. Ozbay, J. Crystal Growth 293 (2006) 273.
[11] J.-H. Lee, H.-M. Ko, I.-H. Lee, Y.-J. Park, Y.-H. Lee, M.-B. Lee, S.-H. Hahm, J.-H. Lee, Phys. Status Solidi (c) 1 (2002) 103.
[12] P. Perlin, C. Kisielowski, V. Iota, B.A. Weinstein, L. Mattos, N.A. Shapiro, J. Kruger, E.R. Weber, J. Yang, Appl. Phys. Lett. 73 (1998) 2778.
[13] J. Wu, W. Walukiewicz, K.M. Yu, W. Shan, J.W. Ager III, E.E. Haller, Hai Lu, William J. Schaff, W.K. Metzger, Sarah Kurtz, J. Appl. Phys. 94 (2003) 6478.
[14] M.S. Jeong, Y.-W. Kim, J.O. White, E.-K. Suh, M.G. Cheong, C.S. Kim, H.J. Lee, Appl. Phys. Lett. 79 (2001) 3440.
[15] K. Kim, C.S. Kim, J.Y. Lee, J. Phys.: Condens. Mat. 18 (2006) 3127.
[16] Y.-H. Kim, C.S. Kim, S.K. Noh, S.K. Ban, S.G. Kim, K.Y. Lim, B.S. O, J. Korean Phys. Soc. 42 (2003) S285.
[17] D.E. Aspnes, E.D. Palik (Eds.), Handbook of Optical Constants of Solids, Academic Press, Orlando, 1985, p. 89.
[18] J. Bai, T. Wan, P.J. Parbrook, K.B. Lee, A.G. Cullis, J. Crystal Growth 282 (2005) 290.
[19] LEPTOS User Manual (www.bruker-axs.de), Version 2 (2004).
[20] S. Takaqi, Acta Crystallogr. 15 (1962) 1311;
D. Taupin, Bull. Soc. Fr. Mineral. Crystallogr. 87 (1964) 469.

[21] B. Heying, X.H. Wu, S. Keller, Y. Li, D. Kapolnek, B.P. Keller, S.P. DenBaars, J.S. Speck, Appl. Phys. Lett. 68 (1996) 643.
[22] H. Yu, D. Caliskan, E. Ozbay, J. Appl. Phys. 100 (2006) 033501.
[23] G.B. Stephenson, J.A. Eastman, C. Thompson, O. Auciello, L.J. Thompson, A. Munkholm, P. Fini, S.P. DenBaars, J.S. Speck, Appl. Phys. Lett. 74 (1999) 3326.
[24] A. Jimenez, Z. Bougrioua, J.M. Tirado, A. Brana, F. Calleja, E.E. Munoz, I. Moerman, Appl. Phys. Lett. 82 (2003) 4827.
[25] A. Torabi, P. Ericson, E.J. Yarranton, W.E. Hooke, J. Vac. Sci. Technol. B 20 (3) (2002) 1234.
[26] J. Bai, T. Wang, P. Comming, P.J. Parbrook, J.P.R. David, A.G. Cullis, J. Appl. Phys. 99 (2006) 023513.
[27] T. Aggerstam, S. Lourdudoss, H.H. Radamson, M. Sjödin, P. Lorenzini, D.C. Look, Thin Solid Films 515 (2006) 705.
[28] C.G. Van de Walle, M.D. McCluskey, C.P. Master, L.T. Romano, N.M. Johnson, Mater. Sci. Eng. B59 (1999) 274.